Dimers of the 9-Diazofluorene Anion Radical and Their Behavior†

Donald Bethell*‡ and Vernon D. Parker*⊥

Contribution from the Robert Robinson Laboratories, University of Liverpool, P.O. Box 147, Liverpool, L69 3BX England, and Laboratory for Organic Chemistry, Norwegian Institute of Technology, N-7034 Trondheim-NTH, Norway. *Received June 17, 1985*

Abstract: Derivative cyclic voltammetry (DCV) has been used to investigate further the dimeric species formed when 9-diazofluorene undergoes one-electron reduction in acetonitrile solution. It has been confirmed that, at low substrate concentration (0.25 mM), the anion radical of 9-diazofluorene is sufficiently long lived to be detected voltammetrically before dimerization and ultimate formation of fluorenone azine. DCV experiments conducted at a higher 9-diazofluorene concentration (5 mM) with a rest potential typically at −2.5 V relative to the reference electrode (Ag/Ag^+) permitted voltammetric examination of the species intermediate between 9-diazofluorene anion radical and fluorenone azine. Two dimeric dianion forms of the initial anion radical have been observed, one detectable only at low temperatures (−43 to −24 °C) which undergoes single-step, two-electron oxidation in competition with transformation by loss of nitrogen to the azine dianion, and the other long lived over the temperature range −43 to +41 °C which undergoes two successive quasi-reversible one-electron oxidations and is converted much more slowly into the azine. Possible structures of these dimeric species and their revelance in the electron-transfer chain catalysis of the decomposition of 9-diazofluorene are discussed.

9-Diazofluorene (**1**) on cathodic reduction in aprotic solvents is converted essentially quantitatively into fluorenone azine (**2**) with high current efficiency.[1,2] The mechanism of the reaction and in particular the fate of initially formed anion radicals of **1** has been a topic of some considerable interest and a little controversy. This controversy has centered on the interpretation of cyclic voltammograms of **1** in solution in solvents such as dimethylformamide (DMF) and acetonitrile.

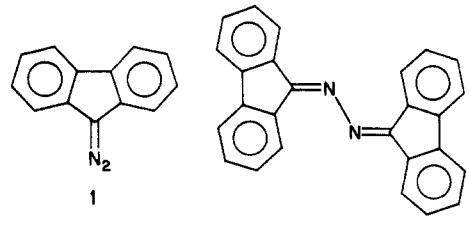

1

2

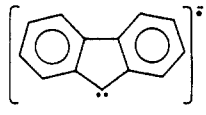

3

McDonald, Hawley, and their co-workers were the first to report[1] cyclic voltammetry of **1** in $DMF/Bu_4N^+ClO_4^-$ at low voltage sweep rates (200 mV s^{-1}). Reduction of **1** was irreversible and on the reoxidation sweep three peaks were observed. For the purposes of this paper we shall number peaks observed in this way 1, 2, 3, etc., in the sequence of decreasing negative peak potential E^p. The values of E_1^p and E_2^p were identical with those observed in the reversible cyclic voltammetry of **2** to $\mathbf{2}^{-\cdot}$ and $\mathbf{2}^{2-}$. Peak 3 which was much less clearly defined than the other two could not be related to any likely product of reaction even though it seemed to form part of a reversible couple. The tentative assignment of it to the carbene anion radical **3** which was thought to be the initial reaction product from $\mathbf{1}^{-\cdot}$ by unimolecular nitrogen loss was challenged[3] on the grounds of the short lifetime of diarylcarbenes,[4] and this threw doubt on the whole interpretation of the reaction.

Reexamination of the cyclic voltammetry of **1** at lower temperatures and sweep rate of 1 V s^{-1} revealed changes in behavior.[3] At −20 °C peak 1 disappeared and peaks 2 and 3 were observed. These had a peak current ratio of close to unity and were reversible. Further lowering of the temperature of −50 °C led to almost total disappearance of both peaks and the appearance of a more intense peak 4 at a less negative potential. The species responsible for peak 4 was not part of a reversible redox couple but gave rise to the couples associated with peaks 2 and 3. Taken in conjunction with kinetic studies[5] of the behavior of $\mathbf{1}^{-\cdot}$ by linear sweep voltammetry (LSV) and double potential step chronoamperometry (DPSC) which showed a second-order dependence of the rate on $[\mathbf{1}^{-\cdot}]$, peak 4 was assigned to a dimer of $\mathbf{1}^{-\cdot}$. Peaks 2 and 3 were assigned to fluorenone azine dianion **4** and anion radical **5**, respectively, both in their cis forms largely because of the similarity in ΔE^p to that for the trans forms observed in CV of **2**. The effect of temperature changes on the cyclic voltammetry was interpreted as arising from partial cis–trans isomerization of the dianions and anion radicals. This interpretation led to the tentative suggestion that the dimer of $\mathbf{1}^{-\cdot}$ might have the novel structure **6** or be $\mathbf{8}^{2-}$.

More recently Herbranson et al.[6] have shown that electrochemical reduction of fluorenone triphenylphosphazine (**7**) leads to P–N bond cleavage and the generation of $\mathbf{1}^{-\cdot}$. CV studies at temperatures of 25 and 1 °C showed peaks on the reoxidation phase corresponding to peaks 2 and 3 in the reduction of **1**. By elegant coulometric/gas-pressure studies they were able to demonstrate that peak 2 corresponded to oxidation of a dimer of $\mathbf{1}^{-\cdot}$ with no loss of nitrogen, peak 3 related to a further one-electron oxidation, whereafter formation of **2** resulted. Under the conditions of the CV experiments, peak 4 was not detected. The dimeric dianion was formulated as arising by head to head linkage of two $\mathbf{1}^{-\cdot}$ forming $\mathbf{8}^{2-}$.

Since the relationship between the species responsible for peaks 2, 3, and 4 remains unclear and since this relationship is intimately related to the mechanism of the electron-transfer chain catalysis of the decomposition of 9-diazofluorene, we have carried out further investigation of the voltammetry of **1** over a wide temperature range in acetonitrile solution using a novel methodology. For comparison the behavior of **7** under similar conditions has

† Intermediates in the Decomposition of Aliphatic Diazo Compounds. Part 21.

‡ University of Liverpool.

⊥ NTH, Trondheim.

(1) McDonald, R. N.; Borhani, K. J.; Hawley, M. D. *J. Am. Chem. Oc.* **1978**, *100*, 995.

(2) Bethell, D.; McDowall, L. J.; Parker, V. D. *J. Chem. Soc., Perkin Trans. 2* **1984**, 1531.

(3) Bethell, D.; Galsworthy, P. J.; Handoo, K. L.; Parker, V. D. *J. Chem. Soc., Chem. Commun.* **1980**, 534.

(4) Closs, G. L.; Rainow, B. E. *J. Am. Chem. Soc.* **1976**, *98*, 8190. For more recent work on fluorenylidene itself see: Griller, D.; Montgomery, C. R.; Scaiano, J. C.; Platz, M. S.; Handel, L. *Ibid.* **1982**, *104*, 6813. Grasse, P. B.; Brauer, B.-E.; Zupancic, J. J.; Kaufmann, K. J.; Schuster, G. B. *Ibid.* **1983**, *105*, 6833.

0002-7863/86/1508-0895$01.50/0 © 1986 American Chemical Society

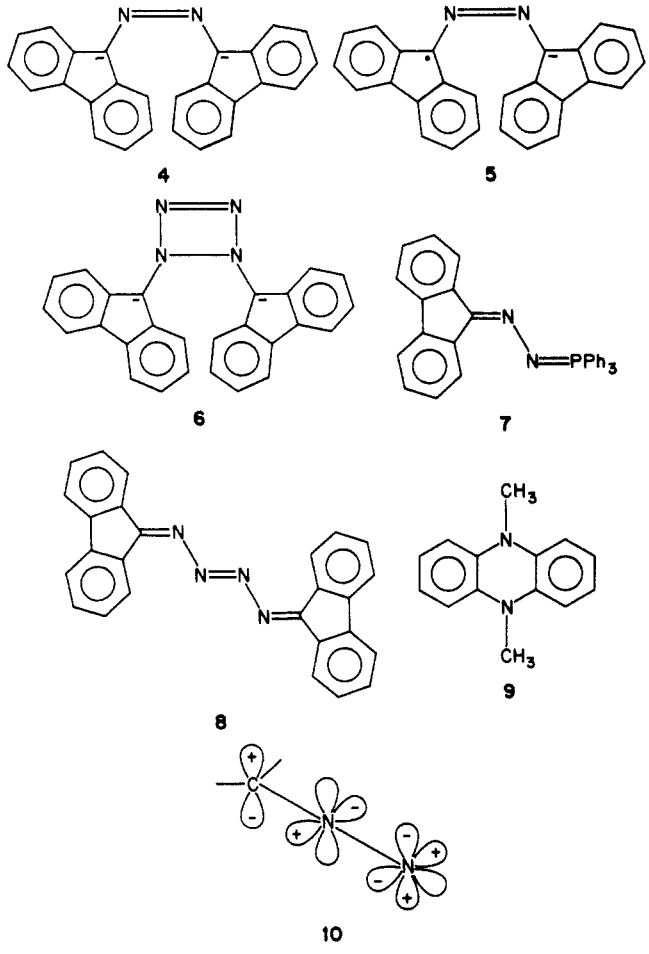

also been examined. The results are in line with our earlier findings in dimethylformamide solution and suggest that $\mathbf{1}^{-}\cdot$ gives rise to two different dimeric species on the reaction path leading to azine.

Results

All experiments described in this paper were conducted in acetonitrile as solvent, containing $Et_4N^+BF_4^-$ (0.1 M), using the techniques of derivative linear sweep and derivative cyclic voltammetry (DLSV and DCV) because of their sensitivity. Unless otherwise noted, the working electrode was platinum and the reference electrode was Ag/Ag^+ (0.01 M in CH_3CN).

Figure 1a represents the first three segments of a 2-cycle derivative cyclic voltammogram for a substance undergoing reversible one-electron reduction. The first segment, from the starting potential (E_{st}) to the switching potential (E_{sw}), is the first derivative of the first half of an ordinary cyclic voltammogram. The height of the peak, like that in ordinary cyclic voltammetry, is proportional to the substrate concentration. The potential at which the curve passes through zero defines the reduction peak potential. At E_{sw} the direction of voltage change is reversed and the reverse process is observed on this segment. A new cycle is initiated at E_{st}.

As a preliminary, in order to provide more conclusive evidence that the process $\mathbf{1} + e \rightarrow \mathbf{1}^{-}\cdot$ is indeed detectable by DCV, double cyclic experiments were carried out with use of a mercury electrode. It is conceivable that the peak that we have previously assigned to the oxidation of $\mathbf{1}^{-}\cdot$ could instead be due to the oxidation of a rapidly formed product of $\mathbf{1}^{-}\cdot$. The theoretical two-cycle voltammogram obtained by digital simulation for a reversible electron transfer is shown in Figure 1a. The feature of interest, for this no reaction case, is that the peak due to the forward process (Ox + e → Red) has the same height on the second as on the first cycle. In contrast, if Red is rapidly consumed by a chemical reaction, the peak due to this process is greatly diminished on the second cycle as in Figure 1b. In Figure 1c we show the experimental two-cycle DCV for the reduction of **1** under conditions

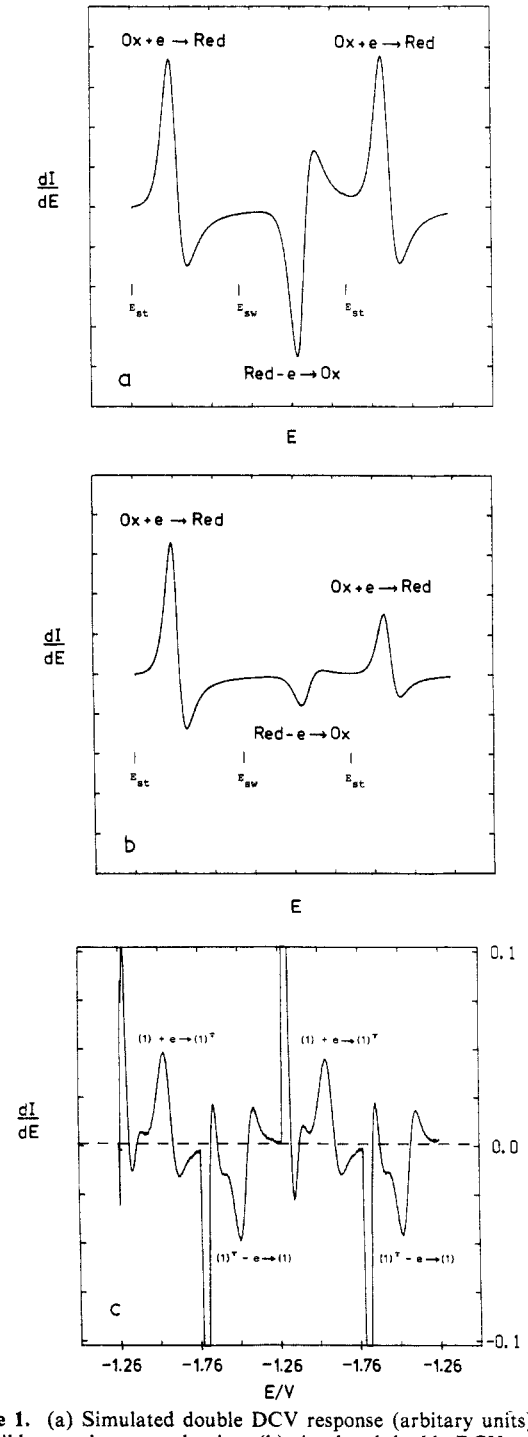

Figure 1. (a) Simulated double DCV response (arbitary units) for a reversible one-electron reduction; (b) simulated double DCV response (arbitrary units) for rapid consumption of the reduced form (Red) of the substrate (Ox); (c) observed two-cycle DCV response for reduction of **1** (0.25 mM) in $CH_3CN/Et_4N^+BF_4^-$ (0.1M) at 16.9 °C; voltage sweep rate 50 V s^{-1}.

where little $\mathbf{1}^{-}\cdot$ is consumed by the formation of dimers. To ensure the latter, a low substrate concentration (0.25 mM), to decrease the rate of the second order reaction, and a relatively high sweep rate (50 V/s) were used. This resulted in the peak for the reduction of **1** on the second cycle being only slightly diminished from that on the first. This shows that **1** is indeed generated on the return scan of the first cycle and provides strong support for our previous assignment. The peaks at the start and switching points in Figure 1c, i.e., those at −1.26 and −1.76 V, are due to changes in the double layer charging current as the scan is started and reversed and should be ignored when comparisons are made with theoretical voltammograms (Figure 1, a and b) which do not take into account the double layer charging current.

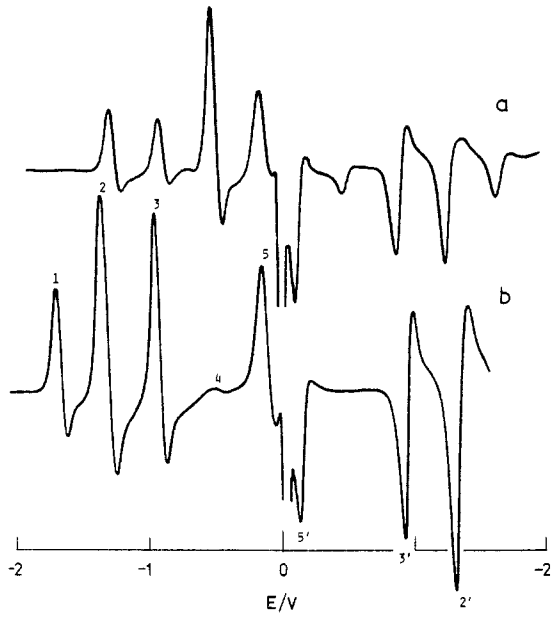

Figure 2. Derivative linear sweep voltammograms showing the oxidation of products derived from diazofluorene anion radical in acetonitrile–$Et_4N^+BF_4^-$ (0.1 M) at a Pt electrode at 100 V s^{-1}: (a) −43 °C; (b) −13 °C.

To study the effect of temperature on the formation of dimers of $\mathbf{1}^{-\cdot}$ we adopted a different methodology in which, with a 5 mM solution of **1**, the rest potential of the working electrode was made large and negative so that in the diffusion layer **1** was completely converted to $\mathbf{1}^{-\cdot}$ and thence to dimeric species. This then allowed us to examine the DCV behavior of the dimers, without interference from **1** and $\mathbf{1}^{-\cdot}$ as a function of temperature.

Figure 2 shows typical DCV traces between −2.0 and 0 V from a rest potential of −2.5 V for acetonitrile solutions of **1** containing 9,10-dimethyl-9,10-dihydrophenazine (**9**) (0.67 mM). Peaks 1–4 are due to dimers of $\mathbf{1}^{-\cdot}$ while peak 5 is for the oxidation of **9** included as an internal standard. At −43 °C peak 1 was not observed. Peaks 2 and 3 correspond to those assigned by McDonald and Hawley to the (linear) dimer of $\mathbf{1}^{-\cdot}$. The dominant feature is, however, the peak labeled 4 for which E^p = -0.40 V. This corresponds with the peak previously reported in the low-temperature CV of **1** in DMF.[3] It should be noted that on the return sweep the relative heights of the derivative current peaks 4′, 3′, and 2′ are quite different from those of 4, 3, and 2. If the oxidation products were stable under the conditions of the measurements the peak height ratios 4′/4, 3′/3, and 2′/2 would all be unity. It is clear that the species responsible for 4/4′ is largely consumed when it is oxidized, giving rise on the cathodic going sweep to 1′ and making the ratio 3′/3 greater than unity. Peak 2′ which arises both from the reduction of a dimeric anion radical and from one-electron reduction of **2** is likewise more intense than peak 2.

At −13 °C a different pattern of behavior is observed (Figure 2b). Peak 1 (E^p = −1.60 V), corresponding to one-electron oxidation of $\mathbf{2}^{2-}$, appears, peaks 2 and 3 are now the most prominent features, and peak 4 is completely absent. Furthermore on the time scale of the experiment, all couples appear to be chemically reversible.

An interpretation of these qualitative findings is that, over the temperature range −43 to −13 °C, the principal route from $\mathbf{1}^{-\cdot}$ to $\mathbf{2}^{2-}$ is by way of the species responsible for peak 4 which also gives rise to the dimer identified by McDonald and Hawley. This dimer appears to be stable and to undergo two successive, reversible, one-electron oxidations.

In an attempt to quantify this treatment, DLSV current ratios R were determined for each of the derivative peaks 1 to 4 relative to that for **9** added in low concentration to the solution. Results are in Table I for eight different temperatures from −45 to +41 °C, and voltage sweep rates from 1 to 100V s^{-1}, although some slower sweeps were carried out at the higher temperatures. While the use of **9** to provide a standard signal permits the estimation of the relative steady-state concentrations of the products of reduction of **1**, the method does not eliminate the effects of diffusion; unlike **9**, the products are not present in appreciable concentrations in the bulk of the solution and diffusion away from the electrode must occur to some extent during the course of the sweep. This effect of R falling with decreasing sweep rate should

Table I. Derivative Current Ratios from DLSV Experiments on the Oxidation of Products from $\mathbf{1}^-$

temp, °C	ν, V s^{-1}	R_1	R_2	R_3	R_4
−45	100		0.99	1.18	2.42
	50		0.86	1.16	2.28
	20		0.69	1.04	2.12
	10		0.62	0.88	2.07
	5		0.52	0.70	2.07
	2		0.35	0.45	1.99
	1		0.24	0.33	1.89
−35	100	0.20	1.10	1.10	1.45
	50	0.18	1.02	1.08	1.51
	20	0.15	0.89	0.94	1.45
	10	0.14	0.77	0.82	1.36
	5	0.15	0.69	0.73	1.30
	2	0.14	0.56	0.58	1.26
	1	0.14	0.48	0.50	1.23
−29.5	100	0.28	1.43	1.41	0.84
	50	0.26	1.29	1.36	0.77
	20	0.23	1.06	1.20	0.64
	10	0.21	0.93	1.06	0.60
	5	0.20	0.84	0.94	0.61
	2	0.17	0.72	0.75	0.63
	1	0.17	0.61	0.63	0.56
−24	100	0.42	1.63	1.70	0.25
	50	0.39	1.38	1.55	0.25
	20	0.35	1.16	1.36	0.23
	10	0.33	1.09	1.27	0.27
	5	0.32	1.04	1.15	0.30
	2	0.32	0.99	1.01	0.31
	1	0.34	0.92	0.92	0.24
−13	100	0.83	1.76	1.59	
	50	0.84	1.58	1.46	
	20	0.84	1.47	1.35	
	10	0.90	1.48	1.31	
	5	0.97	1.55	1.29	
	2	1.10	1.71	1.26	
	1	1.31	1.92	1.31	
0	100	0.96	1.83	1.35	
	50	0.91	1.63	1.27	
	20	0.86	1.50	1.19	
	10	0.86	1.44	1.16	
	5	0.83	1.43	1.15	
	2	1.02	1.56	1.05	
	1	1.16	1.71	0.99	
	0.5	1.38	1.98	0.81	
	0.2	1.90	2.65	0.25	
+17.5	100	0.94	1.54	0.85	
	50	0.97	1.52	0.87	
	20	0.97	1.40	0.82	
	10	0.92	1.35	0.76	
	5	0.93	1.35	0.73	
	2	0.98	1.42	0.66	
	1	1.14	1.60	0.50	
	0.5	1.41	1.99	0.22	
+41	100	1.84	2.35	0.45	
	50	1.78	2.23	0.47	
	20	1.80	2.30	0.58	
	10	1.98	2.48	0.56	
	5	2.07	2.58	0.59	
	2	2.22	2.57	0.50	
	1	2.38	2.78	0.31	
	0.5	2.38	2.92		
	0.2	2.38	2.58		

Table II. Relative Concentrations of Products from $1^{-\cdot}$ in the Diffusion Layer at Steady State

temp, °C	2^{2-a}	A^{2-b}	B^{2-c}	$\Sigma(R/n)$
−45		0.99	1.21	2.20
−35	0.20	1.10	0.73	2.03
−29.5	0.28	1.41	0.42	2.11
−24	0.42	1.70	0.13	2.25
−13	0.83	1.59		2.42
0	0.96	1.35		2.31
17.5	0.94	0.85		1.79
41	1.84	0.45		2.29

[a] R_1. [b] R_3. [c] $R_4/2$.

be least with R_1 and greatest for R_4. At the lowest temperatures, when chemical reactions which might interconvert the species responsible for peaks 1 to 4 will be least important, all R values do indeed fall with decreasing sweep rate in line with this prediction, with peaks 2 and 3 showing the largest effects. At the higher temperatures some values of R show substantial increases as the sweep rate is reduced and this is clear evidence of chemical transformations. We note that the value of ΣR with $\nu = 100$ V s^{-1} is roughly constant over the whole temperature range, and this leads us to suppose that R values at the highest sweep rate do represent a fairly accurate view of the relative concentrations of the reduction products of **1** at the steady state.

The pattern of results that can be discerned from Table I is fairly simple. Peak 4 is dominant at the lowest temperature on both fast and slow voltage sweeps, but its importance declines rapidly and monotonically with temperature and above −24 °C is absent. Peak 3, however, increases in importance with increasing temperatures up to −24 to −13 °C under which conditions its decrease on lowering the sweep rate is minimized. Further increase in temperature sees peak 3 decline and the sweep rate effect increase somewhat. Peak 1 attributable to one-electron oxidation of 2^{2-} is absent at −45 °C, increasing steadily in prominence as the temperature is raised. Decreasing the sweep rate leads to a reduction in R_1 up to −13° whereafter it increases dramatically. Peak 2 is composite, measuring the importance both of $2^{-\cdot}$ and a dimeric dianion. R_2 increases steadily over the whole temperature range while at the same time the diminishing effect of decreasing the sweep rate declines in importance.

Peaks 1–4 arise from five distinct species. Peak 1 arises from the oxidation of 2^{2-} to $2^{-\cdot}$; peak 2 has contributions from $2^{-\cdot} \rightarrow$ **2** and oxidation of a dimer of $1^{-\cdot}$ [which we shall refer to as A^{2-}] to $A^{-\cdot}$; peak 3 is due to $A^{-\cdot}$ going to A and peak 4 is due, we believe, to another dimer of $1^{-\cdot}$, which we designate B^{2-}, undergoing two-electron oxidation to B. Evidence for the two-electron oxidation follows from the following analysis of the data of Table I (see Table II). At the rest potential (−2.5 V) the species present near the electrode surface are 2^{2-}, A^{2-}, and B^{2-} in concentrations that are characterized by R_1/n_1, R_3/n_3, and R_4/n_4 where n refers to the number of electrons transferred in the corresponding oxidation step and the R values are those obtained at the highest voltage sweep rate. The sum $R_1/n_1 + R_3/n_3 + R_4/n_4$ should be constant under steady-state conditions at -2.5 V over the temperature range studied, and this is found to be so if $n_1 = n_3 = 1$ and $n_4 = 2$. Table II gives the values of R/n as a function of temperature.

For comparison, a second series of experiments was performed in which fluorenone triphenylphosphazine (**7**; 1.5 mM) was the substrate in place of **1**. In this case, the rest potential chosen was −3.0 V and sweeping the voltage to zero at 41 °C showed only peaks 2 and 3 at all sweep rates faster than 1 V s^{-1}. Slower sweep rates showed the appearance of peak 1. The data are in Table III. The observations are in line with the earlier CV observations of Herbranson et al.[6] in DMF solution. The results point to a rather slow transformation of A^{2-} to 2^{2-} even at 41 °C, and they

(5) Parker, V. D.; Bethell, D. *Acta Chem. Scand.* **1980**, *B34*, 617; **1981**, *B35*, 691.

(6) Herbranson, D. E.; Theisen, F. J.; Hawley, M. D.; McDonald, R. N. *J. Am. Chem. Soc.* **1983**, *105*, 2544.

Table III. Derivative Current Ratios from DLSV Experiments on the Oxidation of Products from $7^{-\cdot}$ at 41 °C

ν, V s^{-1}	R_1	R_2	R_3
100		0.300	0.283
50		0.321	0.302
20		0.306	0.291
10		0.341	0.310
5		0.332	0.305
2		0.287	0.245
1	0.026	0.214	0.152
0.5	0.032	0.135	0.086

Scheme I[a]

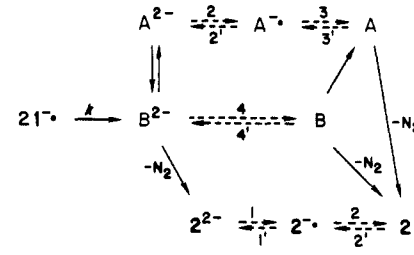

[a] Broken arrows indicate electrochemical steps, the numbers beside them referring to the corresponding peaks observed in DLSV and DCV experiments.

contrast sharply with the results obtained under similar conditions using **1** as the substrate, where 2^{2-} is the dominant product. The conclusion that the dimer A^{2-} is not the principal precursor of 2^{2-} under the present conditions seems inescapable.

Discussion

We interpret our observations in terms of Scheme I in which solid arrows refer to chemical steps and broken arrows to electrochemical ones. Chemical transformation of A- or B-species into **2** or its reduced forms has been represented as irreversible since it necessarily entails loss of molecular nitrogen.

The processes following heterogeneous charge transfer at the electrode surface begin with the dimerization of $1^{-\cdot}$ for which the rate constant k is 1.3×10^5 M^{-1} s^{-1} at 13 °C.[5] The structure of the dimer formed initially is unknown and may or may not be the first observable intermediate, B^{2-}.

The results of Table II are consistent with Scheme I. At the lowest temperature B^{2-} is the dominant species present and in the range from −45 to −24 °C its importance declines as the steady-state concentrations of A^{2-} and 2^{2-} increase. The evidence of Figure 2 makes it clear that oxidation of B^{2-}, followed by a further rapid cathodic sweep, leads to an increase in signals due to the A-series and **2** and its reduction products. At a temperature of −13 °C, the B-series of dimeric species is no longer present and further increases in temperature continue to affect the relative amounts of A-species and **2**.

The linear dimer A^{2-} is converted to the azine dianion slowly even at 41 °C (Table III). Peak 1, due to oxidation of 2^{2-}, was only observed at sweep rates equal to 1 V/s or lower. In contrast, dimers formed from the reduction of **1** are converted to azine at temperatures as low as −35 °C and rapidly at 0 °C and above (Table I). The data suggest that all **2** observed at sweep rates greater than 1 V/s arise from the B-species and at higher sweep rates the ratio R_3/R_1 gives the relative rate constants for the formation of A-species and **2**. This being the case, the difference in activation energies for the formation of the two can be obtained from a correlation of log R_3/R_1 as a function of $1/T$. A plot of the data in Table I measured at 100 V/s (Figure 3) results in a difference in Arrhenius activation energies of 6 kcal/mol, with the formation of 2^{2-} having the higher value.

Both A-species and 2^{2-} could arise either from the same intermediate or by independent routes. The fact that the proportion of A-species present goes through a maximum at about −24 °C while the proportion of B-species steadily decreases and 2^{2-} increases suggests that the B-species is indeed the precursor of both A-species and **2**.

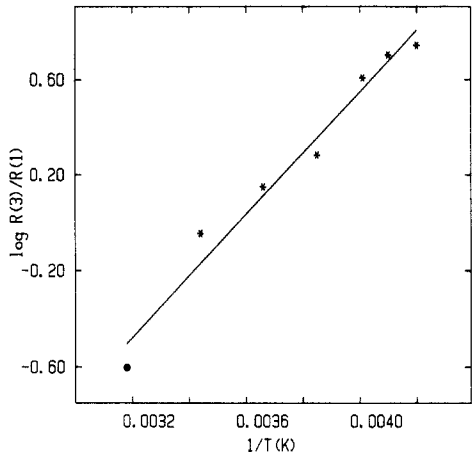

Figure 3. Arrhenius plot of the variation of the ratio of derivative current ratios R_3/R_1 with temperature. The correlation line (r = 0.97) corresponds to ΔE = 5.9 kcal/mol, $\Delta \log A = -4.6$.

The Structure of the Dimers. The electrochemical observations that we have described do not in themselves provide any structural information. Values of E_1^P, E_2^P, and E_3^P are, however, separated by fairly constant voltages which suggests that the relationship of 2^{2-} to $2^{-\cdot}$ to **2** is rather similar to that between A^{2-}, $A^{-\cdot}$, and A. This suggests that there might be a structural similarity between A and **2** and this would be in line with the views of McDonald and Hawley that A is a linear dimer of **1**.

The only experimental evidence about the nature of B^{2-} and B is their chemical behavior and the value of E_4^P, which falls in the range of potentials associated with the oxidation of carbanions and was the justification for our tentative formulation of B^{2-} as **6** in our earlier publications. The experimental observation that B^{2-}, unlike A^{2-}, undergoes two-electron oxidation and readily loses molecular nitrogen to form 2^{2-} is clearly of structural significance.

To proceed further we need to consider the electronic structure of $1^{-\cdot}$. Reduction of **1** involves the introduction of an electron into its LUMO and for diazo compounds this will be the in-plane N–N π^* orbital.[8] The effect of the reduction will be to produce an anion radical, the structure of which can be approximated by **10**, with the odd electron essentially localized on the terminal nitrogen atom in a p-type orbital lying in the plane of the molecule. Dimerization is thus expected to occur through the terminal nitrogen atoms to produce an approximately planar tetrazinyl dianion. An analogy is to be found in the diffusion-controlled dimerization of phenyldiazenyl radicals produced in the pulse radiolysis of benzenediazonium ions which yields a linear tetrazadiene.[9] It can be envisaged that in the present work the tetrazinyl dianion could exist in cisoid and transoid forms as shown in **11** and **12**, the cisoid conformer being of higher energy.[10] A close analogue of the cisoid conformer is employed in 1,4′-diaryltetrazadiene complexes of a range of transition metals (e.g., Fe) although there the aromaticity of the tetrazametallocycle is thought to play a part.[11] Such a cisoid species would be set up for thermal conrotatory electrocyclic ring closure to produce **6** which is formally a 6 π-electron ring and from which loss of nitrogen might be expected to proceed readily. The ready loss of nitrogen from **11** or **12** is not so easily envisaged.

Other dimeric structures can be written (e.g., **13**), but these entail combination of an anion radical **10** with one in which the odd electron is associated with the out-of-plane π system, in turn

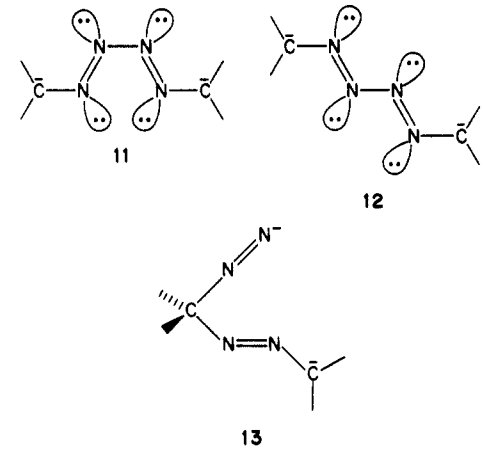

requiring the electron to be introduced into a higher energy π orbital than the LUMO. For this reason and because the structure **13** would be expected to lose nitrogen so readily that it probably would not be detectable by DCV, we dismiss this structure. In our view A^{2-} is most probably the transoid dimer **12** as suggested by Herbranson et al.[6] It seems unlikely that B^{2-} is the corresponding cisoid conformer **11** for the following reasons: (i) The cisoid dimeric dianion would be expected to undergo two successive one-electron oxidation steps as does A^{2-} rather than a single two-electron oxidation as observed for B^{2-}. (ii) The potentials at which A^{2-} and B^{2-} are oxidized (peaks 2 and 4 in Figure 2) differ by approximately 750 mV which is very much larger than is observed in the redox behavior of cis and trans isomeric pairs (e.g., stilbene[12]). The different redox behavior of A^{2-} and B^{2-} could be accounted for if the two are conformers of the same species provided that the extent of π conjugation in A^{2-} is significantly greater than in B^{2-}. The delocalization of the charges in B^{2-} would have to be similar to that in the 9-fluorenyl anion since their oxidation potentials are nearly the same. However, we incline to the view that a mere conformational difference could not account for the ease of nitrogen loss from B^{2-} compared with A^{2-}.

The cyclic structure **6** which should readily lose N_2, especially on removal of two electrons, is consistent with all of our observations on B^{2-}: However, we retain the reservations which we voiced previously,[5] concerning the strain in such a structure and the difficulty of formulating electronic arguments that would predict its formation from $1^{-\cdot}$. Earlier,[5] we considered a linear dimer as a more likely candidate for B^{2-} but we now believe that A^{2-} has that structure and we know that it yields azine only slowly. Thus, in spite of our reservations, we can see no preferable alternative to structure **6** for B^{2-}.

Our previously reported[3] observations on the electrochemical reduction of **1** labeled with ^{15}N at N^{α} have a further bearing on the interpretation. Examination of the azine produced under conditions of constant potential electrolysis showed that 8 ± 4% of the product carried two ^{15}N labels consistent with formation via **6**. The remainder was found to be singly labeled. The experiments were conducted at ca. 20 °C, conditions under which we would expect (i) any of the dimer B^{2-} formed would be transformed into A^{2-} + 2^{2-} and (ii) reaction of $1^{-\cdot}$ with **1** would be expected to be competitive with dimerization. The latter reaction might be expected to yield either $A^{-\cdot}$, assuming no loss of nitrogen, or $2^{-\cdot}$. Our earlier interpretation of the ETC decomposition of **1** as involving electron transfer from the chain carrier to **1** in the rate-determining step suggested that the species responsible for peak 3 could be the chain carrier, since it had an oxidation potential appropriate to explain the observed rather slow chain-propagation rate. To be compatible with the labeling result, however, the resultant product **8** would have to lose predominantly two nitrogen atoms situated at the end of the chain of four; loss of the central two would lead to doubly labeled **2**. However, attack

(7) Ahlberg, E.; Svensmark, B.; Parker, V. D. *Acta Chem. Scand.* **1980**, *B34*, 53. Ahlberg, E.; Parker, V. D. *J. Electroanal. Chem.* **1981**, *121*, 57. Parker, V. D. *Adv. Phys. Org. Chem.* **1983**, *19*, 131.

(8) Jorgensen, W. L.; Salem, L. "The Organic Chemist's Book of Orbitals"; Academic Press: New York, 1973; p 126.

(9) Brede, O.; Mehnert, R.; Naumann, W.; Becker, H. G. O. *Ber. Bunsenges. Phys. Chem.* **1980**, *84*, 666.

(10) Dale, J. "Stereochemistry and Conformational Analysis"; Universitetsvorlaget/Verlag Chemie: Oslo/Weinheim, 1978; p 113.

(11) See, for example, Trogler, W. C.; Johnson, C. E.; Ellis, D. E. *Inorg. Chem.* **1981**, *20*, 980.

(12) Jensen, B. S.; Lines, R.; Pagsberg, P.; Parker, V. D. *Acta Chem. Scand.* **1977**, *B31*, 707.

of $1^{-\cdot}$ on **1** would not necessarily lead to the same nuclear arrangement as dimerization of $1^{-\cdot}$ and the question of the structure of the chain carrier and its chemical behavior on electron transfer must remain open.

Experimental Section

Materials. 9-Diazofluorene (**1**) was prepared as previously described.[13] The phosphazine **7** was prepared by reaction of **1** with triphenylphosphine in acetonitrile solution; recrystallized from chloroform/ether it had mp 209-210 °C (lit.[14] mp 209-210 °C). Acetonitrile and tetraethylammonium tetrafluoroborate were purified commercial samples; solutions (0.1 M) were dried immediately prior to addition of **1** or **7** by filtration through a 20-cm column of activated alumina (Woelm, N. Super).

DCV and DLSV Experiments. The instrumentation was as described in earlier publications.[15] The working elecrode was a platinum disc 0.4 mm in diameter and the reference electrode Ag/Ag^+ (0.01 M in CH_3CN). Solutions of **1** (5 mM) or **7** (1.5 mM) containing 9,10-dimethylphenazine (0.67 mM) were studied. The starting potential for experiments on **1** was -2.5 V and the scan was +2.5 V at intervals of 60 s; experiments on **7** started at a potential of -3.0 V and the scan was +3.0 V. After differentiation of the current-voltage curves and analog to digital conversion, the peak height ratios were evaluated with an on-line computer. The standard deviations on the values was usually 1% of the quoted value.

Registry No. 1, 832-80-4; **7**, 751-35-9; triphenylphosphine, 603-35-0.

(13) Staudinger, H.; Kupfer, O. *Ber.* **1911**, *44*, 2197.
(14) Staudinger, H.; Meyer, J. *Helv. Chim. Acta* **1919**, *2*, 619.
(15) See, for example: Parker, V. D. *Acta Chem. Scand.* **1981**, *B35*, 349.

Structural and Magnetic Study of $Ni_2(EDTA)(H_2O)_4,2H_2O$. Alternating Landé Factors in a Two-Sublattice 1D System

E. Coronado,[⊥] M. Drillon,*[⊥] A. Fuertes,[‡] D. Beltran,[‡] A. Mosset,[§] and J. Galy[§]

Contribution from the Dépertement Science des Matériaux, E.N.S.C.S., 67008 Strasbourg, France, the Departamento de Quimica Inorganica, Universidad de Valencia, Valencia, Spain, and the Laboratoire de Chimie de Coordination, du C.N.R.S., 31400 Toulouse, France.
Received January 25, 1985

Abstract: We report on the structure and magnetic behavior of the chain complex $Ni_2(EDTA)(H_2O)_4,2H_2O$ characterized by two different sites for Ni(II) ions. These are coordinated either to the EDTA ligand or to oxygen atoms belonging to carboxylate groups of the EDTA and four water molecules; they are connected in order to form alternating zigzag chains. The magnetic behavior is discussed in terms of regular spin-1 chain with alternating Landé factors $S(g_a)$-$S(g_b)$-$S(g_a)$.... Both Heisenberg and Ising exchange models are shown to describe the experimental data down to about 10 K, for a coupling constant $J \simeq -8.3$ K. However, due to local anisotropy effects, the latter gives a better agreement with experiment at lower temperature.

Thermodynamics of one-dimensional Heisenberg systems was first investigated by Bonner and Fischer[1] in a pioneering work on the spin $^1/_2$ chain and extended by Weng[2] and De Neef[3] to higher spin networks. Further, the $S = {}^1/_2$ dimerized chain involving two exchange parameters was solved by Duffy and Barr[4] by means of the same computational procedure. Results of these studies were extensively confronted with experiment, so that they constitute today current methods when determining the exchange constants in 1D materials.[5] When discrepancies occur at low temperatures these are usually attributed either to interchain couplings or to distortions of the local environments leading to a splitting of the low-lying levels. Unfortunately, a complete treatment of such effects is not available so far.

Recently, we have shown that the alternation of magnetic sites (two-sublattice chain) due to distinct local symmetries or distinct metal ions causes equally drastic effects on the temperature dependence of the effective moment.[6-8] Mention, in particular, a minimum of the curve $\chi T = f(T)$ at intermediate $kT/|J|$ value and a divergence when approaching absolute zero, according to a power law variation. Such a behavior was shown to be the signature of a ferrimagnetic short-range ordering.

In this paper, we discuss the structure and magnetic properties of the $Ni_2EDTA(H_2O)_4,2H_2O$ complex showing two distinct nickel(II) sublattices connected in order to form infinite chains A-B-A-B.... From an electronic viewpoint, the site symmetry alternation results in alternating Landé factors, and consequently in alternating moments. Then, the problem is to be compared to the previously investigated one on the ordered bimetallic chains with two distinct spin sublattices. The behavior of the title compound will be discussed here on the basis of Heisenberg and Ising chain models including a g alternation.

Table I. Crystallographic Data and Conditions for Data Collection and Refinement

1. Physical and Crystallographic Data

formula: $Ni_2(C_{10}N_2O_8)(H_2O)_4,2H_2O$ molecular weight: 513.73
crystal system: orthorhombic space group: $Pna2_1$
a = 14.370 (25) Å V = 1821.2 Å^3
b = 9.638 (5) Å Z = 4
c = 13.150 (5) Å
ρ_{expt} = 1.86 (2) g·cm^{-3}; ρ_X = 1.87 g·cm^{-3}

2. Data Collection

temperature: 20°C
radiation: molybdenum $\lambda K\bar{\alpha}$ = 0.71069 Å
monochromatization: oriented graphite crystal
crystal-detector distance: 208 mm
detector window: height* = 4 mm; width* = 4 mm
take-off angle: 2°
scan mode: θ-2θ
maximum Bragg angle: 27°
scan angle: $\Delta\theta = \Delta\theta_0 + B \tan\theta$; $\Delta\theta_0$ = 0.90, B = 0.347
values determining the scan-speed: SIGPRE* = 0.75; SIGMA* = 0.018; VPRE* = 10°/mn; TMAX* = 90 s
controls: intensity orientation
reflections: $00\bar{4}$, $\bar{4}00$, $0\bar{6}0$; 060, 415, 008
periodicity: 3600 s; 100 reflections

3. Conditions for Refinement

reflections for the refinement of the cell dimensions: 25
recorded reflections: 2291
utilized reflections: 1956 with $I \geq 3\sigma(I)$
refined parameters: 253
reliability factors: $R = \sum||k|F_o| - |F_c||/\sum k F_o = 0.033$; $R_w = [\sum w(k|F_o| - |F_c|)^2/\sum wk^2F_o^2]^{1/2} = 0.040$

[⊥] Dépertement Science des Matériaux, E.N.S.C.S.
[‡] Universidad de Valencia.
[§] Laboratoire de Chimie de Coordination, du C.N.R.S.

0002-7863/86/1508-0900$01.50/0 © 1986 American Chemical Society